RISING AND BOUNCING BUBBLES AGAINST A BOUNDARY WITH BEM; THE EFFECT OF VISCOUS STRESSES

Evert KLASEBOER[1*], Rogerio MANICA[1] and Derek CHAN[2]

[1] Institute of High Performance Computing, SINGAPORE, 138632
[2] The University of Melbourne, VIC 3010, Australia

*Corresponding author, E-mail address: evert@ihpc.a-star.edu.sg

ABSTRACT

It is well known that the Boundary Element Method (BEM) based on potential flow theory is an ideal model to simulate high Reynolds number flows. However, for rising bubbles viscous effects can no longer be neglected since drag forces will ultimately have to compensate the buoyancy force for a terminal velocity to set in. We present a method to include viscous effects in the boundary element method for high Reynolds numbers, based on a model by Joseph and Wang (2004). The model takes into account surface tension effects and was used to predict the terminal velocity and the shape of millimetre sized bubbles in a pure system (Duineveld, 1995; Klaseboer et al. 2011) with good agreement.

Subsequently, this model is used to predict the bouncing of a bubble against a surface. A thin film between the bubble and the (horizontal) boundary builds up a pressure that pushes the bubble back. A comparison with experimental data (Zawala et al. 2007) shows excellent agreement, including shape oscillations that occur just after the rebound. For bigger bubbles, several bounces are observed before the bubble settles at the solid boundary.

The current framework leads to rapid simulation times as compared to other numerical methods, yet containing all the essential physics of the problem and could lead to a better understanding of problems involving bubbles in many industrial applications in terms of bouncing and coalescence behavior.

NOMENCLATURE

g	gravity acceleration	p	pressure
r	radial coordinate	z	vertical coordinate
u	velocity		
κ	surface curvature	ρ	density
ϕ	velocity potential		
σ	surface tension	μ	dynamic viscosity

1. INTRODUCTION

Potential flow theory alone is known not to be able to predict rising bubbles, due to the fact that the drag force is not modelled. A way to introduce viscous effects in potential flow for the rising bubble problem was given by Klaseboer et al. (2011). They implemented the viscous pressure and the viscous normal stress condition at the bubble-water interface based on a model by Joseph and Wang (2004).

Often potential flow problems are solved using a boundary element method (BEM). These methods have the advantage of mesh reduction (only a mesh on the bubble is needed) and thus the bubble can be followed relatively easily as compared to other numerical methods that use fixed spatial grids.

Thin films have been the focus of research for decades (Scheludko 1957, Chan et al. 2011). It is now understood that the thin film generates a pressure that can cause the rebound of a bubble (Klaseboer et al. 2001; Hendrix et al. 2012). For most cases, the film is so thin that lubrication theory entirely dominates the flow physics in the film, even though the flow outside the film region might be mainly dominated by high Reynolds number flow phenomena. This realization opens the possibility to model such systems in a smart manner. In his review on numerical methods in free-surface flows Yeung (1982) said: "*The 'best' numerical methods to come may well be those that exploit analytical simplifications that are appropriate for the physical phenomenon being examined.*" The current article is written with this idea in mind; we keep the important aspects of the problem through physical insight. In the Section 2 the numerical model will be described, followed by predicting the terminal velocity of a bubble in Section 3. Then the rebound of a soap bubble (Section 4) and a bubble in water (Section 5) are investigated.

2. MODEL DESCRIPTION

The potential of a flow with velocity vector **u** (**u**$=\nabla\phi$) satisfies the Laplace equation:

$$\nabla^2\phi = 0. \tag{1}$$

The pressure due to the potential flow satisfies the Bernoulli equation:

$$p = p_\infty - \rho\frac{\partial\phi}{\partial t} - \frac{1}{2}\rho|\mathbf{u}|^2 - \rho gz. \tag{2}$$

At the bubble surface the pressure makes a jump due to surface tension and other terms:

$$p = p_{bub} - \sigma\kappa + 2\mu\frac{\partial u_n}{\partial n} + p_v + p_{film}. \tag{3}$$

The term $2\mu\partial u_n/\partial n$ represents the viscous normal stress jump across the interface (u_n is the normal component of the velocity). The terms p_v and p_{film} are viscous pressures that result from the fact that the fluid is not entirely behaving as potential flow (in pure potential flow the drag

force would always be zero). The term p_v originates from the boundary layer around the bubble and the term p_{film} originates from the pressure that builds up when the bubble is close to a boundary. Both of these terms will be explained shortly. The pressure inside the bubble p_{bub} is taken adiabatically (except for the section on the soap bubble, where another potential flow is assumed inside the bubble):

$$p_{bub} = p_0 \left(V_0 / V \right)^\gamma \qquad 4)$$

With $p_0 = p_{ref} + 2\sigma/R$ (p_{ref} = 1 Bar and R is the initial bubble radius), V and V_0 are the volume and initial volume of the bubble respectively. The exponent γ is taken as 1.25. The curvature of the bubble κ, is implemented as in Chesters (1977), where the two radii of curvature on the axisymmetric bubble surface are determined as

$$\kappa = \kappa_1 + \kappa_2 = \frac{\sin\Omega}{r} + \frac{d\sin\Omega}{dr}, \qquad 5)$$

where Ω is the tangent angle which is related to the normal vector as: $\mathbf{n} = \left(-\sin\Omega, \cos\Omega \right)$.

An axial symmetric implementation of the boundary element method has been used.

$$c\phi(\mathbf{r}_0) + \int \phi(\mathbf{r}_0) \partial G(\mathbf{r}, \mathbf{r}_0)/\partial n \, dS = \int G(\mathbf{r}, \mathbf{r}_0) \partial \phi(\mathbf{r}_0)/\partial n \, dS$$
$$6)$$

with the Green function $G(\mathbf{r}, \mathbf{r}_0) = 1/|\mathbf{r}_0 - \mathbf{r}|$ and c the solid angle at location $\mathbf{r}_0$.

We apply a method based on Joseph and Wang (2004) to estimate the viscous pressure p_v at the bubble surface (assuming a high Reynolds number flow). This pressure originates from the fact that potential flow alone will neglect the boundary layer that will build up around the bubble. According to them, the viscous pressure must compensate for the non-zero shear stress τ at the bubble surface. They derived an exact integral expression as:

$$-\int (\mathbf{u} \cdot \mathbf{n}) p_v \, dS = \int (\mathbf{u} \cdot \mathbf{t}) \tau \, dS \qquad 7)$$

For a spherical bubble an exact solution can be derived. In our calculations we assume that the bubble can still be approximated by a sphere and take $p_v \approx C\cos(\beta)$, where $0 < \beta < \pi$ is the normalised arc length of the bubble surface. From the above integral equation the constant C can be determined and thus p_v is known. More details on the implementation can be found in Klaseboer et al. (2011).

Another contribution that is not represented by potential flow is the pressure that builds up in the thin film separating the bubble and the boundary. There are two aspects to this pressure, the first one associated with the energy stored due to the deforming surface (surface tensions acts like a spring), the second one is the viscous damping in the film. We assume that the pressure is a function of the deformation alone (thus ignoring any viscous losses) and behaves as simple power law:

$$p_{film} = \sigma / R \left(d / z \right)^4 \qquad 8)$$

Where d is a constant set to be $0.1R$ (the exact value does not appear to have much influence on the results as long as $d << R$, but not too small to cause numerical problems, i.e. $d >$ meshsize). A fourth order dependence on the z-coordinate is chosen to create a 'steep' enough barrier, such that only the film region experiences the film pressure (as is the case in a real bouncing bubble problem, Klaseboer et al. 2001) and the film pressure decays rapidly everywhere outside the film region. The position $z = 0$ corresponds to the rigid boundary (if present). Imposing a pressure in the above form will neglect viscous dissipation

in the film, yet will model the energy storage due to surface tension. In practice, the film will flatten until a pressure almost equal to the Laplace pressure $2\sigma/R$ has been built up in the film. A recent article by Hendrix et al. (2012) revealed the complex behaviour of the film region during bubble impact on a rigid surface.

The potential of the bubble surface is updated with a discretized version of the Bernoulli equation, rewritten as:

$$\rho \frac{D\phi}{Dt} = -p + \frac{1}{2}\rho|\mathbf{u}|^2 - \rho g z + p_{ref} \qquad 9)$$

Note that $D\phi/Dt = \partial\phi/\partial t + \mathbf{u} \cdot \nabla\phi = \partial\phi/\partial t + |\mathbf{u}|^2$. The position of the bubble interface is updated with $D\mathbf{r}/Dt = \mathbf{u}$ at each time step. Then the potential is calculated with the above equation and the Boundary Element Method is used to calculate the normal velocity. The tangential velocity can be obtained from the potential distribution along the bubble surface (which is known). The full velocity vector $\mathbf{u}$ is then known and the process can be repeated for the next time step.

In all the simulations, the liquid at infinity is assumed to be at rest. A number of 51 nodes (50 elements) were used on the bubble surface for all the simulations shown here. BEM has the distinct advantage of being very flexible especially for moving bubble problems such as the ones studied here. Only the bubble surface needs to be meshed, which greatly simplifies the tracking of the bubble as it moves and deforms. Furthermore, the computational resources required for the BEM are very modest and the simulation time takes just a few minutes on a PC.
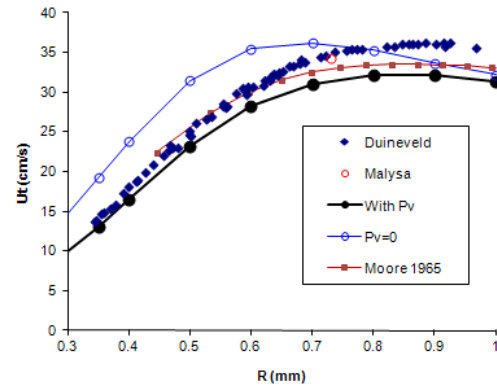
Figure 1: Terminal velocity of a rising 'clean' bubble as a function of the bubble radius R; experimental data of Duineveld (1995) and Malysa et al. (2005) compared with the model with and without p_v term. Also indicated are the theoretical results of Moore (1965). The results with p_v slightly under-predict the experimental results of Duineveld (1995), and when p_v is neglected, they over-predict the terminal velocity for most radii.

3. RESULTS FOR RISING (FREE) BUBBLES

A first test of the model is to calculate the terminal rise velocity and deformation for a bubble far from any walls and under extremely clean conditions (no surface active contaminants). More details can be found in Klaseboer et al. (2011). The results are repeated here in Figs. 1 and 2. The model under-predicts the terminal velocity slightly (Figure 1) but gives excellent agreement for the shape of the bubble (at its terminal speed, Figure 2). Bubbles with

radii smaller than 1.0 mm have been chosen in order to avoid the region where the bubbles move in a zig-zag or spiral manner (a path - instability sets in for larger bubble sizes, which is still poorly understood and outside the scope of the current theory).

In Figures 1 and 2 the results are also shown if p_v is set to 0. This would produce a bubble that has a too high terminal velocity. The term $2\mu\partial u_n/\partial n$ was retained in the simulations. If the contribution $2\mu\partial u_n/\partial n$ would also have been neglected, no drag would exist on the bubble and it would continue to accelerate without reaching a terminal velocity. This indicates that the term p_v does indeed contribute considerably to the drag.
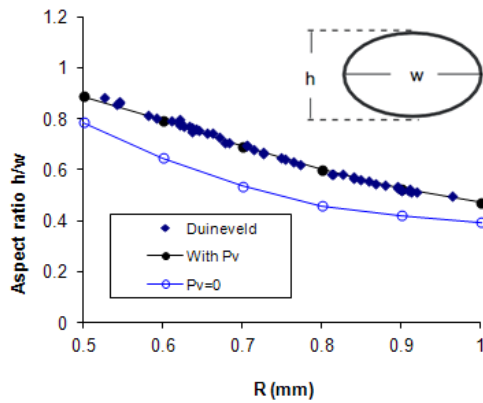
Figure 2: Aspect ratio (definition see inset) of the rising bubble for different bubble radii at terminal velocity. The results with p_v coincide with the experimental results of Duineveld (1995). When p_v is neglected, the model is clearly under-predicting the aspect ratio.

4. "SOAP" BUBBLES BOUNCING AT A WATER INTERFACE

To exploit the possibilities of the developed model, we will first investigate the case of a bouncing soap bubble on a flat stationary water interface (C.V. Boys 1920; Vincent et al. 2007). Since the density of the air inside the bubble is equal to the density of the air outside the bubble, the inertia of the gas inside the bubble cannot be ignored (the added mass of the bubble is of the same order of magnitude as the mass of the gas in the bubble). Vincent et al. (2007) reasoned that the mass of the thin liquid film between the soap surfaces was negligible. In our simulations we have also ignored this mass. A potential flow model using two fluids with two coupled potential flows is now used (Klaseboer and Khoo 2004). The normal velocity and pressure are coupled as boundary conditions for two equations of the type 1 and 2 (one for each flow). In order to simplify the model, the effects of viscosity are here ignored for this case, thus p_v=0 and μ=0. Yet the film pressure p_{film} and surface tension effects are maintained in the model.

The air density is taken as ρ = 1.2 kg/m³. The surface tension of one soap-water interface was measured to be 25 mN/m. Since there are two soap-water interfaces in the bubble, the value for σ is taken to be 50 mN/m for this case. The water surface is assumed to be non-deforming (rigid) during the impact. This is justified since the density

of water is about 1000 times larger than the air in which the bubble moves.

The surface is implemented using an image method through a modified Green function as:

$$G(\mathbf{r},\mathbf{r}_0)=1/\left|\mathbf{r}_0-\mathbf{r}\right|+1/\left|\mathbf{r}_0-\mathbf{r}'\right|,$$

where $\mathbf{r}'$ is the image of point $\mathbf{r}$ in the boundary. The initial conditions for the potential are (inside and outside, corresponding to the potential solution for the motion of a solid sphere):

$$\phi_{out}=-U\cos(\beta)/2$$
$$\phi_{in}=U\cos(\beta)$$

where U is the initial velocity (as given by the experimental data).
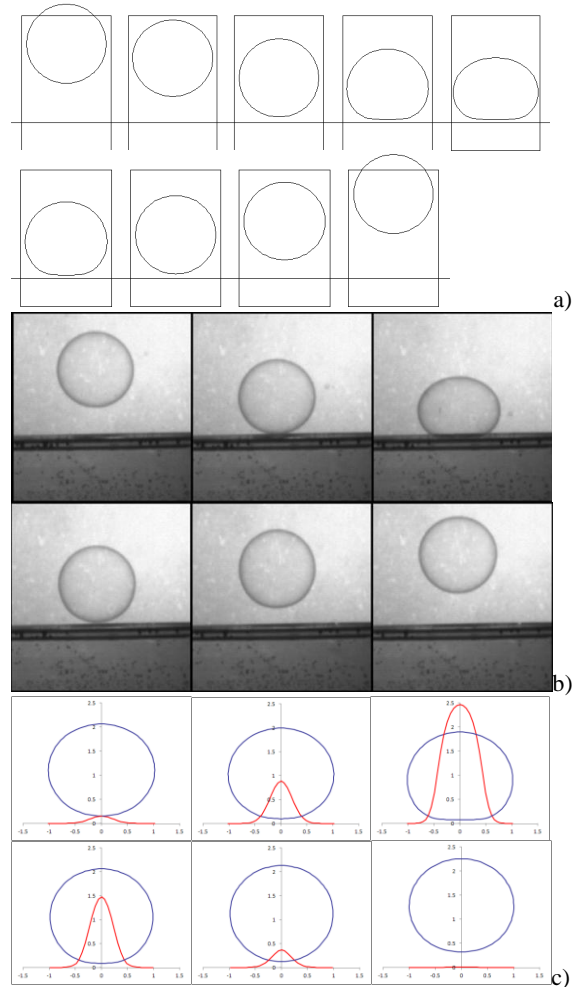
Figure 3: Soap bubble with initial radius 1.1 cm approaching a pool of water with 65 cm/s from t=0 to 50 ms. First rows: approach. Second rows: rebound. a) Numerical results. A rectangular reference frame is drawn around the bubble such that the deformation can be better observed. The horizontal line is the water surface. b) Experimental results t=0 to 70 ms (images reproduced from Vincent et al. 2007). The 'contact time' is ~25 ms in the numerical results and around 30 ms in the experiments. c) Numerical results with pressure in the film indicated in red at the instants t=7.6, 9.1, 11.4, 25.9, 27.4 and 30.5 ms after the start of the simulation.

Two cases were simulated; a bubble with initial radius R=1.1 cm approaching at U=65 cm/s (Figure 3) and a bubble of 0.6 cm radius approaching at 120 cm/s (Figure

4). The results show a very good agreement between the theory and the experimental results (without any adjustable parameters).

The film pressure is absolutely necessary to get the correct physics; otherwise no repulsive force on the bubble will be present that is capable of causing a rebound.

In Figure 3c the pressure in the film is also indicated for several time instants. The maximum pressure reaches about $2.5\sigma/R$ (the Laplace pressure is $2\sigma/R$). These profiles resemble Figure 9 of Klaseboer et al. (2001), or Figure 5 of Klaseboer et al. 2000. In both cases, the pressure in the film also became slightly larger than the Laplace pressure in the bubble. Although smaller, the bubble of Figure 4 is deformed much more (Frame 5) due to its larger initial velocity than the bubble of Figure 3. The pressure build up generates a force on the bubble that is essentially responsible for the observed rebound.

a)

b)
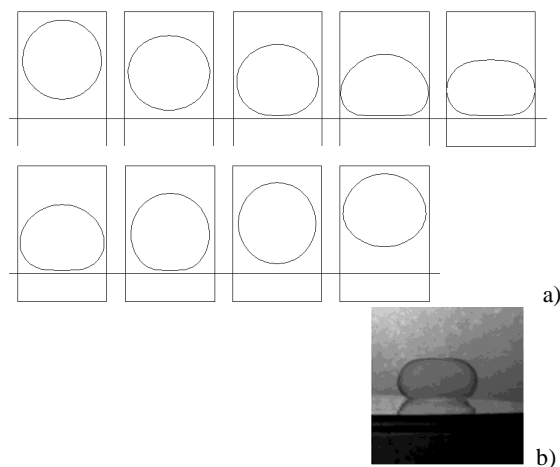
Figure 4: Soap bubble with initial radius 0.6 cm approaching a pool of stagnant water with 120 cm/s. a) Numerical results, time increases from left to right; compare 5th frame with image experimental frame. b) Experimental results (image reproduced from Vincent et al. 2007); only an image of the most deformed state is available for this experiment.

5. "WATER" BUBBLES BOUNCING AGAINST A SUBMERGED RIGID PLATE

Experimental data of Zawala et al. (2007) are now used to test our model under more severe conditions, namely that of an air bubble approaching a flat horizontal submerged surface under ultra pure conditions. The challenge here is not only to get the terminal velocity correct during the pre-bounce period (as in Section 3), but also to predict the bouncing behaviour. Since the inertia of water is much higher than that of air, it is expected that the inertial terms will play a much greater role in the bouncing dynamics.

The image method is again used to model the flat plate. The bubble contents are modelled with Equation 4 (since the density of the air is much less than that of water, there is no need to model the flow inside the bubble with another potential flow as in Section 4). We thus allow (very small) volume changes of the bubble to occur. Both the viscous pressure (Equation 7) and the film pressure (Equation 8) are taken into account.

In Figure 5 a bubble approaching a flat submerged wall is shown with initial terminal velocity = 35 cm/s

(experimental). Our model gives a terminal velocity of ~31 cm/s. The radii of both the experimental and numerical bubble are $R = 0.735$ mm. The frames are taken at exactly the same instant for the experiment (right) and the numerical model (left). Remarkable agreement can be observed indicating that the physics of the model are implemented correctly. The model also predicts violent oscillations that result from inertia and surface tension but could not be predicted with the simpler point force model of Klaseboer et al. (2001). The bubble hits the wall at almost terminal speed (Figure 5a and 5b). It does not seem to slow down much before the very last moment it reaches the wall. The top then flattens considerably (Figure 5c). The bubble then bounces back while exhibiting shape oscillations (Figure 5e to 5g). The bubble bounces back several bubble radii before slowing down and reversing its trajectory once more. In Figure 5h and 5i the second approach is shown. A second rebound occurs in Figure 5j.

Due to the fact that damping in the film was neglected, the numerical bubble bounces back slightly more and thus a slight time delay between the experiment and the simulation can be observed. If a more realistic model is needed, the full lubrication equations must be solved (such as in Klaseboer et al. 2001). Although this can be done, the implementation would be more troublesome, since a mesh for the film and the potential flow must be generated and pressures must be transferred from one model to the other (remember that the film thickness usually is in the micrometer order of magnitude, which was recently confirmed experimentally in Hendrix et al. 2012).

DISCUSSION AND CONCLUSION

Through clever insight it is possible to simulate bouncing bubbles, including viscous effects without any adjustable parameters using the Boundary Element Method. Both a bouncing soap bubble and a bubble in water were simulated. For the soap bubble viscous effects were negligible, but the flow inside the bubble had to be taken into account. For the 'water bubble', viscous effects had to be included. The pressure resulting from the thin film was also modelled as a 'spring-like' pressure; that is, the pressure as implemented in Equation 8 only stores energy, but is not able to simulate viscous dissipation in the film. The fact that this does not have a discernable effect on the results when compared to experiments, indicates that film dissipation is of minor importance and can be neglected (at least in the cases investigated).

Due to the fact that the BEM calculates the whole fluid domain, added mass effects are automatically included in the simulations. Added mass effects will occur during strong accelerations of the fluid, such as will be the case during the impact of bubbles on rigid plates.

The simulation times using the BEM are several minutes for each case as compared to many hours for other methods.

Figure 5: The bouncing 'water' bubble at different instants (each frame plotted at corresponding time; left numerical, right experimental results from Zawala et al. 2007) for a bubble with initial radius R=0.735 mm and fluid viscosity μ=1.0 mPa s. a) and b) approach phase at terminal velocity. c) and d) strong flattening of the bubble. e), f) and g) rebound phase with violent shape oscillations. h) and i) second approach. j) second rebound. The cross with the red dot indicates the experimental centre of mass which is also plotted on the numerical data.

5

REFERENCES

D'ALEMBERT, (1752), "Essai d'une nouvelle théorie de la résistance des fluides", Paris.

BOYS C.V, (1920) "Soap-bubbles, their colours and the forces which mould them", London (first appeared in 1890).

CHAN D.Y.C, KLASEBOER E, MANICA R, (2011) "Film drainage and coalescence between deformable drops and bubbles", *Soft Matter* **7**, 2235-2264

CHESTERS, A.K, (1977), "An analytical solution for the profile and volume of a small drop or bubble symmetrical about a vertical axis". *J Fluid Mech*, **81**, 609-624.

DUINEVELD P.C, (1995), "The rise velocity and shape of bubbles in pure water at high Reynolds number", *J Fluid Mech*, **292**, 325-32.

HENDRIX M.H.W, MANICA R, KLASEBOER E, CHAN D.Y.C, OHL C.-D, (2012) "Spatiotemporal evolution of thin liquid films during impact of water bubbles on glass on a micrometer to nanometer scale" *Phys. Rev. Lett.* (accepted for publication).

JOSEPH D.D, WANG J, (2004), "The dissipation approximation and viscous potential flow", *J Fluid Mech,* **505**, 365-377.

KLASEBOER E, CHEVAILLIER J.-P. GOURDON C, MASBERNAT O, (2000), "Film drainage between colliding drops at constant approach velocity; experiments and modeling", *J.Colloid Int. Science*. **229**, 274-285.

KLASEBOER E, CHEVAILLIER J.-P, MATÉ A, MASBERNAT O, GOURDON C, (2001), "Model and experiments of a drop impinging on an immersed wall", *Physics of Fluids* **13**, 45-57.

KLASEBOER E, KHOO B.C, (2004), "An oscillating bubble near an elastic material", *J.Applied Physics,* 96, 5808-5818.

KLASEBOER E, MANICA R, CHAN D.Y.C, KHOO B.C, (2011) "BEM simulations of potential flow with viscous effects as applied to a rising bubble", *Eng. Analysis with Boundary Elements,* **35**, 489-494.

MALYSA K, KRASOWSKA M, KRZAN M. (2005), "Influence of surface active substances on bubble motion and collision with various interfaces", *Adv Colloid Interface Sci,* **114-115**, 205-25.

MOORE D.W, (1965), "The velocity of rise of distorted gas bubbles in a liquid of small viscosity". *J Fluid Mech,* **23**, 749-66.

SCHELUDKO A, (1957), "Über das Ausfließen der Lösung aus Schaumfilmen", Colloid & Polymer Science **155**, 39-44.

VINCENT F, Le GOFF A, LAGUBEAU G, and QUÉRÉ D., (2007), "Bouncing bubbles", *J. Adhésion*, **83**, 897-906.

YEUNG R.W, (1982), "Numerical methods in free-surface flows", Ann. Rev. Fluid Mech, **14**, 395-442.

ZAWALA J, KRASOWSKA M, DABROS T, MALYSA K, (2007), "Influence of bubble kinetic energy on its bouncing during collisions with various interfaces", *Canad. J. Chem. Engineering*, **85**, 669-678.